


Cite this: *RSC Adv.*, 2025, 15, 14079

# Effects of perfluoropyridine incorporation into poly(hydroxyethyl methacrylate)<sup>†</sup>

Jason Pulfer,<sup>a</sup> Alban Duhamel,<sup>b</sup> Maxime Colpaert,<sup>c</sup> Tim Storr<sup>a</sup> and Chadron M. Friesen<sup>\*d</sup>

Perfluoropyridine (PFP) is a heavily fluorinated heterocycle which readily undergoes nucleophilic aromatic substitution ( $S_NAr$ ) reactions at low temperatures. Herein, we report a facile synthesis of 2-hydroxyethyl methacrylate derivatives of PFP through solvothermal and mechanochemical means. The resulting monomers were polymerized to form hard, insoluble materials which offer an improvement in thermal stability compared to the starting alcohol. Most unusually the 4-substituted PFP-methacrylate derivative displays superior thermal properties in air compared to nitrogen and generally superior thermal properties compared to the starting alcohol. Additionally, di-substitution of the PFP to form the di-methacrylate appears to initiate decomposition of the monomer into ethylene glycol dimethacrylate through an acyl fluoride-mediated transesterification.

Received 17th March 2025  
Accepted 17th April 2025

DOI: 10.1039/d5ra01927c

rsc.li/rsc-advances

## 1. Introduction

Fluoropolymers are ubiquitous in industry and confer properties such as chemical and thermal resistance, anti-wetting and antibiofouling properties, low friction coefficients, and high durability due to the strength of the C–F bond (485 kJ mol<sup>−1</sup>).<sup>1</sup> Fluoropolymers have many applications in areas such as membranes,<sup>2</sup> energy harvesting,<sup>3</sup> sensors,<sup>4,5</sup> biomedical applications,<sup>6–8</sup> protective coatings, seals, gaskets, and automotive hosing.<sup>9</sup> Materials which confer fluorinated properties with low overall fluorine content are attractive due to the current concern regarding per- and polyfluoroalkyl substances (PFAS), and strategies to achieve low-fluorine content polymers are interesting from an academic perspective.

Perfluoropyridine (PFP) is a fluorinated heterocycle which is readily synthesized from commercial feedstocks at high temperatures (see Scheme 1).<sup>10,11</sup> Further work has been done to replace the PCl<sub>5</sub> with Cl<sub>2</sub> as a simpler feedstock.<sup>12</sup>

Notably, this provides a route to a heavily fluorinated material that does not require direct fluorination, making PFP a fluorinated building block with a safer and more economic barrier of entry. PFP has been used to develop a nucleophilic fluoride ion reagent,<sup>13</sup> deoxyfluorinates carboxylic acids to their

corresponding acyl fluorides,<sup>14</sup> is a protecting group for phenols,<sup>15</sup> undergoes reductive hydrodefluorination in the 4-position with hydrogen,<sup>16</sup> and has utility in cross-coupling reactions.<sup>17,18</sup> PFP undergoes nucleophilic aromatic substitution reactions ( $S_NAr$ ) in a highly regioselective, stepwise manner (see Fig. 1).<sup>19</sup>

Utilizing this type of reaction, it is possible to achieve mono-, di-, and tri-substituted derivatives of PFP. The regioselectivity for the initial mono-substitution is explained through DFT calculations by Fuhrer *et al.*, where the energy of the transition state is significantly less in the *para* position *versus* the *ortho* and *meta* positions (see Fig. 2).<sup>19</sup> The HOMO is delocalized across the carbons except for the *para* position, creating an anti-bonding node which can undergo nucleophilic substitution.

Friesen *et al.* demonstrated mechanochemical substitution of PFP in a ball mill at 80 Hz with a cesium carbonate matrix, providing a solvent-free methodology towards the substitution of PFP with a variety of phenolic and alkyl alcohol groups.<sup>20</sup> The resulting pre-polymers undergo further  $S_NAr$  chemistry with glycols to form block copolymers with favorable thermal properties and anti-wetting behaviors. Polymers containing PFP have also been synthesized by utilizing lithium reagents to make carbon-rich polyarylene materials,<sup>21</sup> thio-ene reactions to form thermoset networks,<sup>22</sup> thermal degradation of azides to form azo-linked networks,<sup>23</sup> azide-alkyne “click” chemistry thermosets,<sup>24</sup> and condensation polymers with bisphenols.<sup>25</sup>

Perfluoropyridine has been utilized extensively in thermoset network polymers and condensation polymerizations but has not to our knowledge been applied towards radical polymerizations as a fluorinated “tag.” PFP has been incorporated into monomers to develop materials with high chemical and thermal stability and low glass transition temperatures ( $T_g$ ).

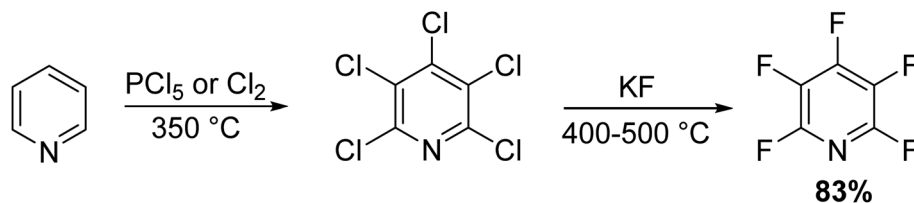
<sup>a</sup>Department of Chemistry, Simon Fraser University, 8888 University Drive, V5A 1S6, British Columbia, Canada

<sup>b</sup>Université de Montpellier, Institut Universitaire de Technologie de Montpellier-Sète, 99 Avenue d'Occitanie, 34090, Montpellier, France

<sup>c</sup>ICGM, University of Montpellier, CNRS, ENSCM, Montpellier, France

<sup>d</sup>Department of Chemistry, Trinity Western University, 22500 University Drive, V2Y 1Y1, British Columbia, Canada. E-mail: chad.friesen@twu.ca

<sup>†</sup> Electronic supplementary information (ESI) available. See DOI: <https://doi.org/10.1039/d5ra01927c>

Scheme 1 Commercial route towards the synthesis of perfluoropyridine.

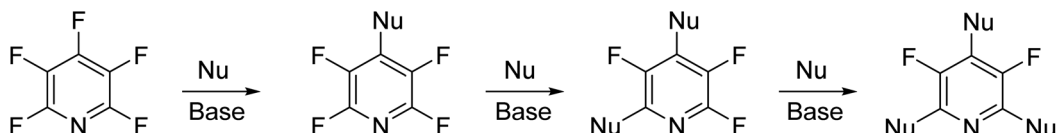


Fig. 1 Nucleophilic substitution patterns in perfluoropyridine.

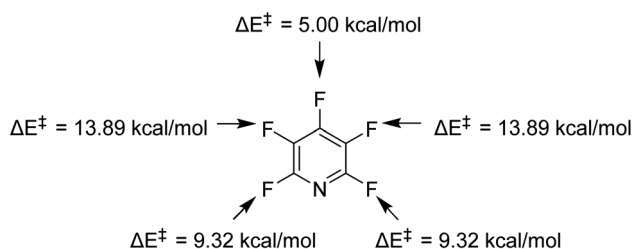


Fig. 2 Transition state energy levels of unsubstituted perfluoropyridine.

Radical polymerizations of PFP-containing substrates would provide insight into the influence of PFP on the thermal stability of polymers, as well as a strategy to mask hydrophilic or nucleophilic components of a molecule such as 2-hydroxyethyl methacrylate (HEMA).

## 2. $S_NAr$ reactions of perfluoropyridine with 2-hydroxyethyl methacrylate

### 2.1. Synthesis of 4-methacryloylethoxy-tetrafluoropyridine

Synthesis of the mono-substituted PFP methacrylate was sought after as a simple substrate to examine the effect of masking a hydrophilic component of a conventional monomer capable

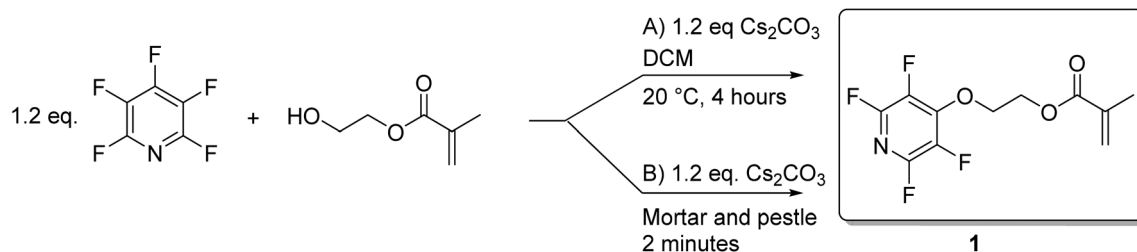
of forming hydrogels. Perfluoropyridine was found to react with 2-hydroxyethyl methacrylate at room temperature, quantitatively converting to the 4-substituted pyridine in 4 hours by  $^{19}\text{F}$  NMR in 83% isolated yield. Since the success of this reaction was evident and inspired by mechanochemical approach based on prior literature,<sup>20</sup> a mortar and pestle were used to synthesize the mono-substituted PFP in quantitative yield by  $^{19}\text{F}$  NMR with 2 minutes of grinding (see Scheme 2).

The monomer displays 2 peaks at  $-90.63$  ppm and  $-158.87$  ppm using  $^{19}\text{F}$  NMR and integrating to equivalent values, indicating 4-substitution of the ring (see Fig. 3).

$^1\text{H}$  NMR displays diagnostic protons at singlet at 6.05 ppm and a triplet at 5.58 ppm for alkene protons, and a triplet at 1.90 ppm for the methyl group of the methacrylate. A doublet of triplets was found at 4.72 ppm and a triplet at 4.50 ppm, corresponding to the protons of the ethylene linker. No alcohol protons were observed, indicating ether formation (see Fig. 4).

Once the monomers had been synthesized and isolated, they were polymerized in the presence of 2,2'-azobis(isobutyronitrile) (AIBN) for 16 hours to ensure complete conversion of the monomer to the poly methacrylate (see Scheme 3).

The resulting polymer (2) was found to be hard, difficult to fragment, and insoluble in all organic solvents. Molecular weight could not be determined as the material was not soluble, and a pressed pellet MALDI-TOF MS spectrum yielded no peaks, indicating resistance to ionization.



Scheme 2 (A) Reaction of PFP with HEMA in the presence of  $\text{Cs}_2\text{CO}_3$  at low temperature, (B) mechanochemical substitution of PFP with methacrylate using a mortar and pestle.



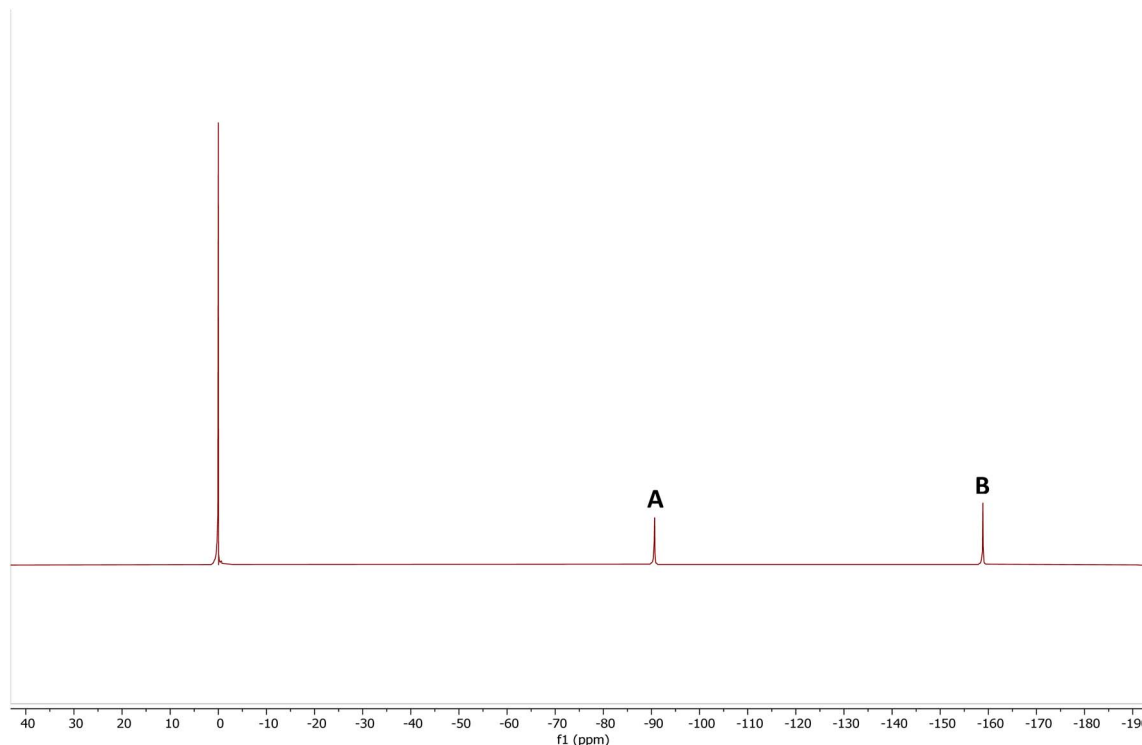


Fig. 3  $^{19}\text{F}$  NMR of the mono-substituted methacrylate product. Reference at 0 ppm is  $\text{CCl}_3\text{F}$ .

## 2.2 Synthesis of 2,4-dimethacroyloxy-3,5,6-trifluoropyridine

After the success of the mono-substituted PFP, the 2,4-disubstituted methacrylate was sought after to examine the thermal effects of multiple methacrylate substitutions. Initially it was thought that the di-substituted derivative was readily attained

through reaction of an excess of methacrylate and base at room temperature (see Scheme 4).

$^{19}\text{F}$  NMR displayed complete conversion to the disubstituted ring, and the product was isolated after alumina filtration as a yellow gelatinous solid at 118% yield relative to PFP. The reason for the unexpected yield will be discussed shortly. Polymerization was observed to proceed readily in bulk to form an

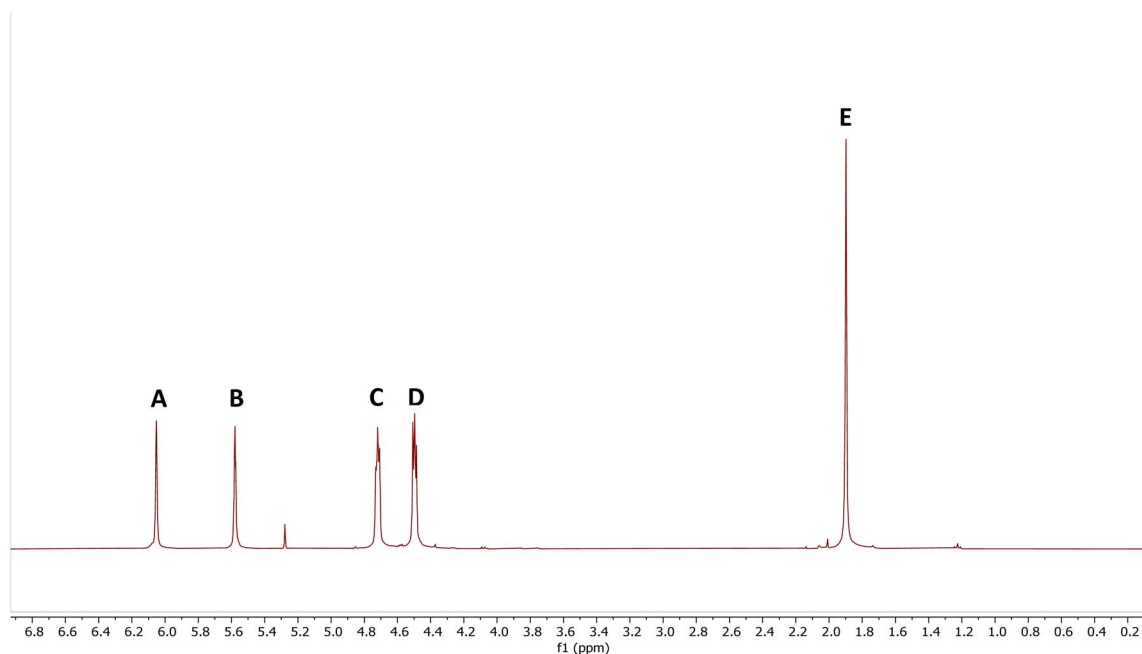
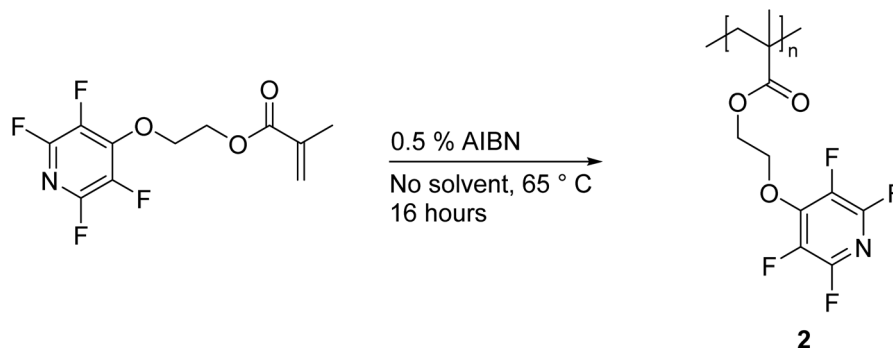


Fig. 4  $^1\text{H}$  NMR of the mono-substituted methacrylate product.



Scheme 3 Bulk polymerization of the 4-PFP-methacrylate.

insoluble species. Complete characterization of **3** after purification yielded some intriguing results.  $^{19}\text{F}$  NMR displays a characteristic pattern of a disubstituted PFP derivative of **3** peaks at  $-93.63$  ppm,  $-159.22$  ppm, and  $-166.12$  ppm all integrating to equivalent amounts (see Fig. 5).

However,  $^1\text{H}$  NMR lacks one of the ethylene protons found in the mono-substituted methacrylate. The  $^1\text{H}$  NMR of the gelatinous product **5** (see Scheme 5) was found to match literature spectra of ethylene glycol dimethacrylate,<sup>26</sup> identifying a surprising product in the reaction with additional equivalents of methacrylate (Fig. 6).

This accounts for the 118% yield relative to PFP which plagued initial scouting reactions and demonstrates that PFP potentially acts as a transesterification reagent in these conditions, echoing past work showing utility of PFP as an amide and ester coupling agent.<sup>14</sup> Realizing there are several product options, the mechanism of this reaction is shown in Scheme 5 and represents possible pathways (see Scheme 5). The initial disubstitution occurs through typical  $\text{S}_{\text{N}}\text{Ar}$  chemistry and the formation of the Meisenheimer complex, which can then undergo acyl substitution with fluoride to generate the acyl fluoride intermediate, and then finally esterification to give **5** as a mixture of final products with **4A** and **4B**. While not the desired product, this indicates that materials with ester functionality should be treated with caution when working with PFP due to its ability to act as a fluoride source, thereby inducing

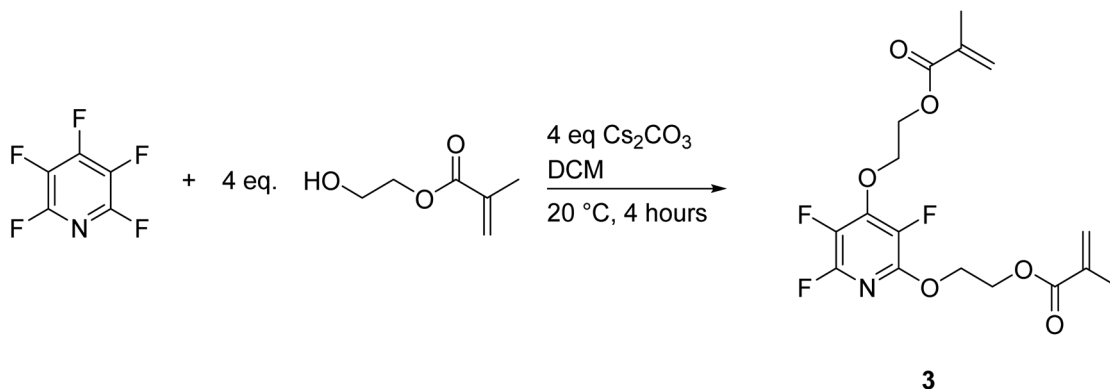
homocoupling. With this in mind, the yield of the homocoupling reaction is 57% isolated yield relative to the **HEMA** component.

The mixture of products **5**, **4A**, and **4B**, were polymerized through reaction with AIBN (see Scheme 6) to give **6**.

### 2.3 Attempted synthesis of 2,4,6-trimethacryloyloxy-3,5-difluoropyridine

Synthesis of the tri-substituted material was significantly more challenging, with no methodology found to successfully provide clean conversion. Heating overnight in tetrahydrofuran (THF) resulted in a solid mass, indicating polymerization occurred.  $^{19}\text{F}$  NMR of the mixture showed no incidence of tri-addition. Addition of (2,2,6,6-tetramethylpiperidin-1-yl)oxidanyl (TEMPO) as a radical scavenger only resulted in di-substitution by  $^{19}\text{F}$  NMR, even after 48 hours of heating (see Scheme 7).

Further reactions with DABCO, DABCO and catalytic cesium carbonate, equimolar equivalents of DABCO and cesium carbonate, higher temperatures up to  $150^\circ\text{C}$  with cesium carbonate, longer reaction times, DMSO as a solvent, and tetrakis(triphenylphosphine) palladium (0) as a metal catalyst failed to provide a successful conversion to the desired product, and either displayed di-addition to the ring or polymerized into a solid mass.



Scheme 4 Synthesis of 2,4-disubstituted PFP with HEMA at low temperature.



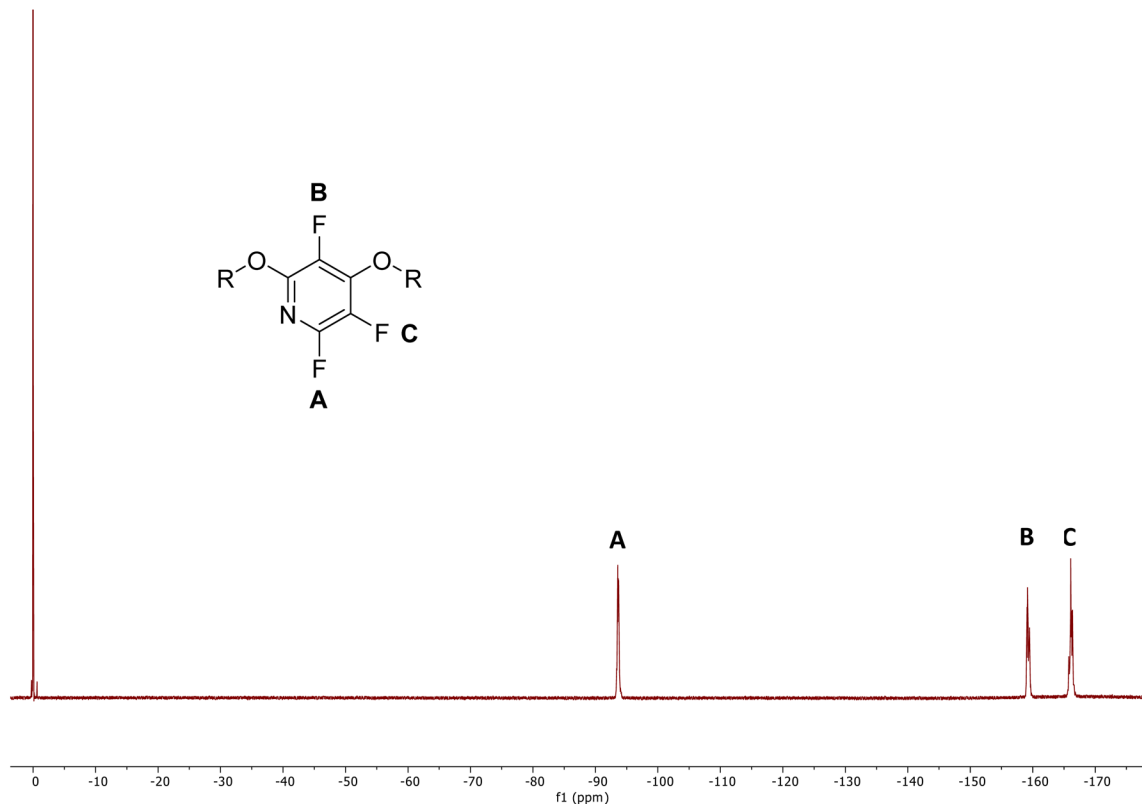


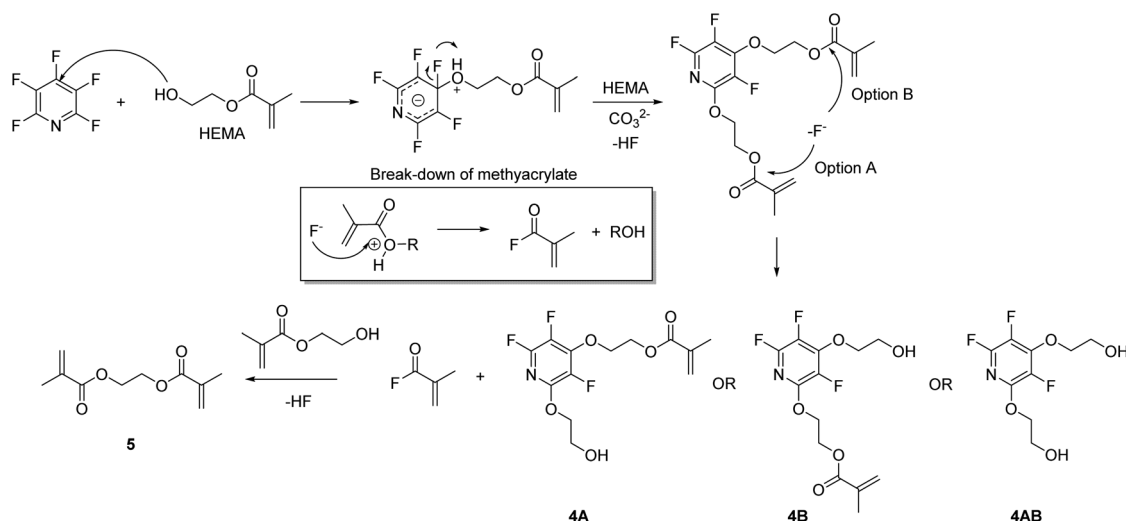
Fig. 5  $^{19}\text{F}$  NMR of the disubstituted ring product **4**. Reference at 0 ppm is  $\text{CCl}_3\text{F}$ .

## 2.4 Molecular weight and thermal analysis

Poly(hydroxyethyl methacrylate) (HEMA) is known to readily form hydrogels.<sup>27</sup> All PFP-containing polymers were insoluble in standard organic solvents but did not display swelling behavior in water to form hydrogels. The monomers were easily characterized by  $^{19}\text{F}$  NMR but show distinct difficulty in acquiring a molecular weight peak. In our hands, MALDI-TOF-MS, EI-MS, ESI-MS, and FD-MS were all unable to provide a molecular

weight peak for the compound, indicating that the material is especially reactive. This is reflected in the difficulty to make tri-substituted variants of the monomers, wherein the material appears to favor polymerization over substitution. Characterization of polymer molecular weight proved impossible in our hands due to the insoluble nature of the material in the case of the mono-PFP derivative.

The  $\text{S}_{\text{N}}\text{Ar}$  reaction can be thought of as a masking of the HEMA alcohol and has an interesting effect on the  $T_{\text{d}}^5$  values.



Scheme 5 Postulated mechanism for the formation of ethylene glycol dimethacrylate from PFP and excess HEMA.

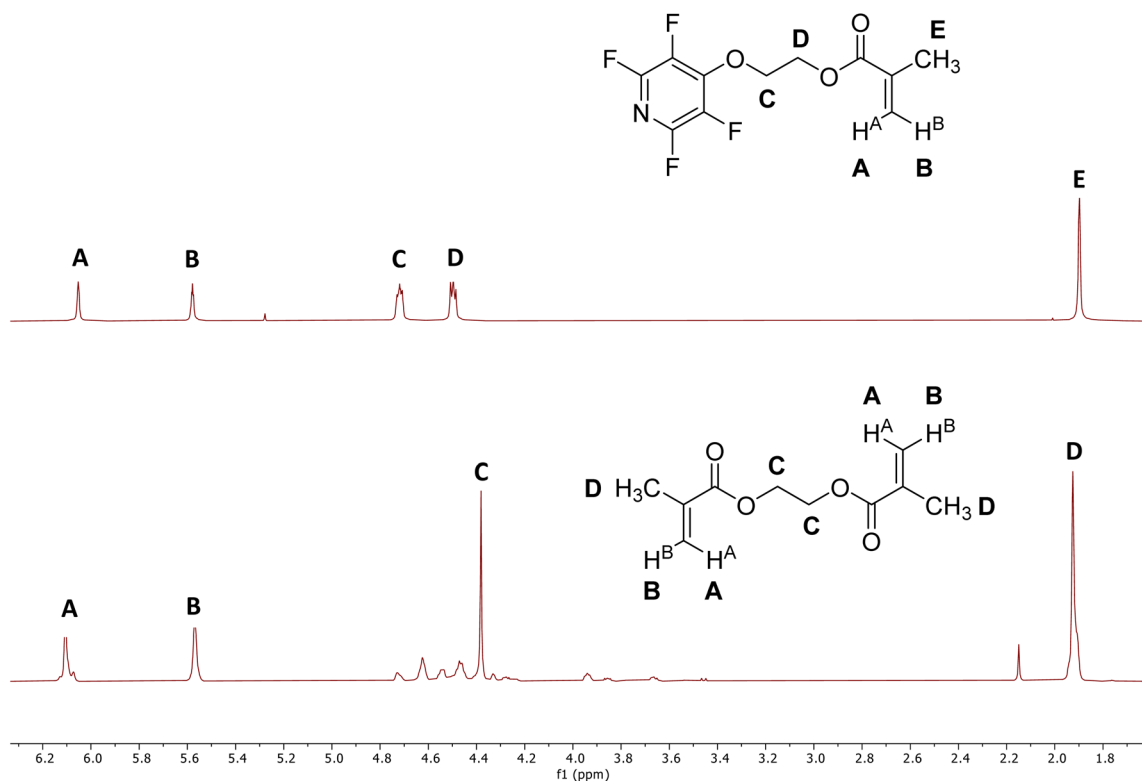
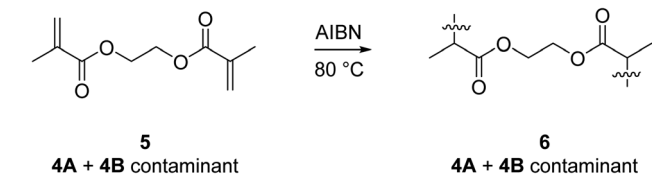


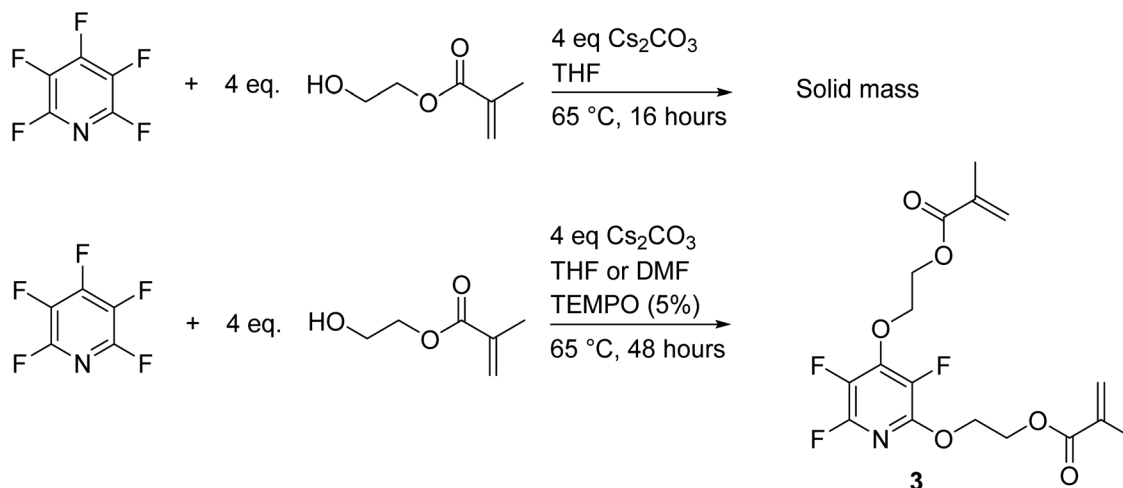
Fig. 6 Comparison of the  $^1\text{H}$  NMR spectrum of 1 (top) and the  $^1\text{H}$  spectra of 5 (bottom).



Scheme 6 Polymerization of the product mixture 5 to produce polymer 6.

PHEMA was synthesized in-house under the same conditions as 2 and 6 to compare thermal data. PHEMA has a  $T_{\text{D}}^{50}$  of 220.6 °C in air, compared to 243.2 °C in nitrogen. Interestingly, 3 increases the degradation temperature by 60.1 °C in air (280.7 °C), but shows a lower degradation temperature (266.9 °C) in a nitrogen atmosphere. 6 also displays a higher  $T_{\text{D}}^{50}$  compared to PHEMA at 267.7 °C but has little disparity ( $\sim 2$  °C) between air and nitrogen atmospheres (see Table 1).

Interestingly, poly (2,2,2, trifluoroethyl methacrylate) (PTFEMA) displays a distinctly higher glass transition temperature ( $\sim 38$ – $91$  °C) compared to that found for both 2 and 4,



Scheme 7 Synthetic attempts towards tri-substitution of PFP with HEMA.





Table 1 Thermal properties of PFP-methacrylates

Polymer	$T_g$ 1 <sup>a</sup> [°C]	$T_g$ 2 [°C]	$T_d^5$ (air) [°C]	$T_d^5$ (N <sub>2</sub> ) [°C]
PHEMA	24.2	—	220.6	243.2
PTFEMA	79.0	—	260.0 (ref. 28) <sup>b</sup>	—
4-PFP-MA (2)	8.1	40.7	280.7	266.9
2,4-PFP-MA (6)	−11.2	—	267.7	265.6

<sup>a</sup>  $T_g$  values were taken after 1 conditioning cycle of the instrument. <sup>b</sup>  $T_d^5$  value taken from the literature.

indicating the bulky fluorinated ring provides a convenient route to reduce the glass transition temperature of polymeric species through PFP integration. It appears the degradation temperatures of about 260 °C are effectively the same between all materials, with the mono-methacrylate showing a ~20 °C advantage in air *versus* nitrogen. Further, PTFEMA displays good solubility in common organic solvents, a property not reflected in the lack of solubility of 2. This indicates some potential morphology which would prevent solubility, leading to potential applications in solvent-resistant coatings. Attempts to melt process 2 only resulted in charring, indicating that the polymer is not amendable to typical polymer processing, and must be cured in a mold for potential applications. AIBN induces bubbling of the material, indicating that applications requiring a clear film or block of material must be cured with an initiator that does not produce gas as a decomposition product, or initiated through purely thermal methods or photocuring.

### 3. Conclusion

Methacrylate derivatives of perfluoropyridine show an increase in decomposition temperature compared to the alcohol precursor, overall increasing thermal stability. In the case of the mono-substituted PFP-methacrylate, the magnitude of thermal stability is increased the most and the resulting material is resistant to typical organic and fluorinated solvents. Tri-substitution of the ring proved impossible in our hands; however thermal analysis indicates the mono-substituted ring is more favorable for higher temperature applications. Further, introduction of **HEMA** to PFP eliminates swelling behavior, indicating that PFP could be used to tune the hydrophilicity of PHEMA-based materials. The mono- and di-methacrylate derivatives of PFP may have applications in solvent-resistant films or coatings. Introduction of PFP into radically polymerizable species may serve as an excellent route to lower glass transition temperatures by a significant margin. Finally, mortar and pestle synthesis of mono-substituted PFP derivatives provides a simple and affordable mechanochemical synthetic strategy which will be expanded upon in future publications.

## 4. Experimental details

### 4.1 Materials

Perfluoropyridine (99%) and cesium carbonate (99.9%), were both used as received from AK Scientific. Dichloromethane (HPLC

grade, ≥ 99.8%), diethyl ether (≥99.0%), and 2-hydroxyethyl methacrylate (≥99%) were used as received from Sigma Aldrich.

### 4.2 Characterization

<sup>19</sup>F, <sup>1</sup>H, and <sup>13</sup>C NMR spectra were collected on a Bruker ASCEND III 400 MHz NMR with a Bruker AVANCE III 400 MHz running TopSpin 3.1.6 and processed using MestReNova. Signals in <sup>1</sup>H (400 MHz) and <sup>13</sup>C NMR (101 MHz) are reported in parts per million relative to an internal standard or CDCl<sub>3</sub> (7.26 ppm for <sup>1</sup>H and 77.16 ppm for <sup>13</sup>C), and <sup>19</sup>F NMR (376 MHz) signals are reported in parts per million with CFCl<sub>3</sub> (0.00 ppm) as an internal standard. Coupling constants are reported in hertz (Hz) to the nearest 0.01 Hz. Multiplicity (the letters s, d, t, q, pent, and sext stand for singlet, doublet, triplet, quartet, pentet, and sextet, respectively).

Attenuated total reflectance Fourier transform infrared spectroscopy (ATR-FTIR) was collected on a ThermoFisher Nicolet 6700 FT-IR Spectrometer fitted with a Smart iTR sampling accessory and reported in reciprocal centimeters (cm<sup>−1</sup>). DSC analysis was carried out using a NETZSCH DSC200F3 calorimeter. The calibration was performed using adamantane, biphenyl, indium, tin, bismuth and zinc standards. Nitrogen was used as purge gas. Approximately 10 mg of sample were placed in perforated aluminum pans and the thermal properties were recorded. Data was analyzed using Proteus 8.1 and OriginPro 2021.

TGA measurements were conducted on a TGA Q50 from TA Analysis. Samples were placed in 30 μL aluminum crucibles and heated from 25 to 500 °C at 10 °C min<sup>−1</sup> under nitrogen or air flow (60 mL min<sup>−1</sup>). Data was analyzed with Origin Pro 2021.  $T^5\%$  was defined as the temperature at which the samples lost 5% of its initial mass.

### 4.3 Synthesis of 4-methacryloylethoxy-tetrafluoropyridine

**4.3.1 Synthesis of 4-methacryloylethoxy-tetrafluoropyridine (1) by solution chemistry.** PFP (3.613 g, 21.4 mmol) was added to a 20 mL scintillation vial with Cs<sub>2</sub>CO<sub>3</sub> (7.287 g, 22.4 mmol), **HEMA** (2.322 g, 17.8 mmol) and diluted with 20 mL DCM. The solution was stirred for 16.5 hours at room temperature in the dark, and reaction conversion was monitored by <sup>19</sup>F NMR. The mixture was diluted in 80 mL DCM, washed 3 × 100 mL H<sub>2</sub>O, dried over MgSO<sub>4</sub>, and concentrated to a clear oil (4.12 g, 83% yield).

<sup>19</sup>F NMR (376 MHz, CDCl<sub>3</sub>, δ): −90.63 (m, PFP 2,6-position C-F), −158.87 (m, 2F, PFP 3,5-position C-F); <sup>1</sup>H NMR (400 MHz, CDCl<sub>3</sub>, δ): 6.05 (s, 1H, R-O(CO)C(CH<sub>3</sub>)CH<sub>2</sub>), 5.58 (m,  $J$  = 1.6 Hz, 1H, R-O(CO)C(CH<sub>3</sub>)CH<sub>2</sub>), 4.72 (m, 2H, PFP-OCH<sub>2</sub>CH<sub>2</sub>O-R), 4.50 (m, 2H, PFP-OCH<sub>2</sub>CH<sub>2</sub>O-R), 1.90 (s, 3H, R-O(CO)C(CH<sub>3</sub>)CH<sub>2</sub>); <sup>13</sup>C NMR (101 MHz, CDCl<sub>3</sub>, δ): 166.99 (s, R-O(CO)C(CH<sub>3</sub>)CH<sub>2</sub>), 147.07 (m,  $J$  = 10.0 Hz, 5.5 Hz PFP 2,6-position C-F), 144.25 (m,  $J$  = 242.2 Hz, 17.2 Hz, 14.4 Hz, 2.8 Hz, PFP 3,5-position C-F), 135.75 (s, R-O(CO)C(CH<sub>3</sub>)CH<sub>2</sub>), 135.26 (m, PFP 4-position *ipso* C-O), 126.45 (s, R-O(CO)C(CH<sub>3</sub>)CH<sub>2</sub>), 72.32 (s, PFP-OCH<sub>2</sub>CH<sub>2</sub>O-R), 62.92 (s, PFP-OCH<sub>2</sub>CH<sub>2</sub>O-R), 18.16 (s, R-O(CO)C(CH<sub>3</sub>)CH<sub>2</sub>).



IR (ATR):  $\nu$  = 2962.32 (w), 2870.36 (w), 1720.73 (m), 1641.73 (m), 1508.74 (m), 1472.49 (m), 1406.77 (w), 1319.43 (m), 1296.67 (m), 1160.85 (m), 1109.02 (m), 1092.13 (m), 970.45 (m), 813.10 (w), 733.72 (w), 695.46 (w), 649.54 (w).

**4.3.2 Synthesis of 4-methacryloylethoxy-tetrafluoropyridine (1) by mechanochemistry.**  $\text{Cs}_2\text{CO}_3$  (0.385 g, 1.18 mmol) was added to a mortar and pestle with PFP (0.202 g, 1.19 mmol) and **HEMA** (0.125 g, 0.96 mmol) and ground for 2 minutes neat. The material was then extracted with  $\text{CDCl}_3$  and the reaction was found to be identical to 1 by  $^{19}\text{F}$  NMR. No PFP was observed by NMR, indicating complete conversion, however evaporative loss is possible in an open system. The mixture was dissolved in 30 mL of DCM, washed with  $3 \times 30$  mL of deionized water, and concentrated to a clear oil (0.094 g, 34% isolated yield).

#### 4.4 Polymerization of 4-methacryloylethoxy-tetrafluoropyridine (2)

1 (2.512 g, 9.0 mmol) was added to a 20 mL scintillation vial with AIBN (10 mg, 0.06 mmol) degassed by freeze-pump-thaw under nitrogen for 3 cycles. The mixture was stirred at 65 °C for 16 hours to ensure complete conversion to the polymer. The material was obtained as a crystalline solid and used without further purification for all forms of analysis (>99% yield).

IR (ATR):  $\nu$  = 2992.44 (w), 2955.75 (w), 2914.73 (w), 1728.36 (m), 1643.63 (m), 1508.97 (m), 1470.73 (s), 1405.98 (m), 1364.77 (w), 1263.22 (w), 1242.53 (w), 1143.26 (m), 113.34 (w), 1088.98 (s), 1041.05 (w), 968.01 (s), 868.01 (w), 745.59 (w) 733.10 (m), 659.52 (w).

#### 4.5 Synthesis of 2,4-dimethacryloylethoxy-trifluoropyridine (3) by solution chemistry

PFP (1.019 g, 6.03 mmol) was added to a 20 mL scintillation vial with  $\text{Cs}_2\text{CO}_3$  (7.815 g, 24.0 mmol) and **HEMA** (3.166 g, 24.3 mmol) and diluted with 6 mL DCM. The solution was stirred for 4 hours at room temperature in the dark, and reaction conversion was monitored by  $^{19}\text{F}$  NMR. The mixture was diluted in 100 mL diethyl ether, washed with 100 mL 1 M NaOH solution,  $3 \times 100$  mL  $\text{H}_2\text{O}$ , 100 mL saturated NaCl solution, and dried over  $\text{MgSO}_4$ . The solution was filtered over Celite and concentrated to a yellow gelatinous solid (2.775 g, 57% isolated yield relative to **HEMA**).

$^{19}\text{F}$  NMR (376 MHz,  $\text{CDCl}_3$ ,  $\delta$ ): -93.63 (m, 1F, PFP 6-position C-F), -159.22 (m, 1F, PFP 3-position C-F), -166.12 (m, 1F, PFP 5-position C-F).  $^1\text{H}$  NMR (400 MHz,  $\text{CDCl}_3$ ,  $\delta$ ): 6.11 (s, 1H, R-O(CO)C(CH<sub>3</sub>)CH<sub>2</sub>), 5.57 (s, 1H, R-O(CO)C(CH<sub>3</sub>)CH<sub>2</sub>), 4.38 (s, 3H, R-O-CH<sub>2</sub>CH<sub>2</sub>-O-R), 1.93 (s, 3H, R-O(CO)C(CH<sub>3</sub>)CH<sub>2</sub>);  $^{13}\text{C}$  NMR (101 MHz,  $\text{CDCl}_3$ ,  $\delta$ ): 167.22 (s, R-O(CO)C(CH<sub>3</sub>)CH<sub>2</sub>), 136.07 (s, R-O(CO)C(CH<sub>3</sub>)CH<sub>2</sub>), 126.10 (s, R-O(CO)C(CH<sub>3</sub>)CH<sub>2</sub>), 62.43 (s, R-O-CH<sub>2</sub>CH<sub>2</sub>-O-R), 18.22 (s, R-O(CO)C(CH<sub>3</sub>)CH<sub>2</sub>).

IR (ATR):  $\nu$  = 2983.71 (w), 2959.61 (w), 2921.17 (w), 1716.62 (m), 1638.03 (m), 1505.36 (w), 1479.03 (m), 1448.21 (m), 1355.46 (w), 1318/26 (w), 1294.30 (w), 1148.43 (m), 1045.73 (w), 942.55 (w), 886.05 (w), 813.37 (w), 736.04 (w), 651.09 (w).

#### 4.6 Polymerization of 2-hydroxyethyl methacrylate

**HEMA** (1.342 g, 10.3 mmol) was added to a 20 mL scintillation vial and AIBN (14 mg, 0.083 mmol) with stirring. The mixture

was heated at 65 °C for 16 hours to ensure complete conversion to the polymer. The material was obtained as a crystalline solid and used without further purification for all forms of analysis (>99% isolated yield).

IR (ATR):  $\nu$  = 3396.04 (b, O-H stretch), 2995.44 (w), 2945.36 (w), 2874.27 (w), 1715.54 (s), 1450.44 (w), 1387.81 (w), 1245.51 (m), 1150.66 (s), 1070.57 (s), 1021.32 (m), 896.81 (w), 847.50 (w), 748.22 (w).

#### 4.7 Polymerization of ethylene glycol dimethacrylate (5) with PFP-ethylene glycol side products (4A+4B)

4 (1.452 g, 3.73 mmol) was added to a 20 mL scintillation vial and AIBN (5 mg, 0.03 mmol) which was mechanically dispersed in the gelatinous solid by stirring with a microspatula. The mixture was heated at 80 °C for 21 hours to ensure complete conversion to the polymer. The material was obtained as a crystalline solid and used without further purification for all forms of analysis.

IR (ATR):  $\nu$  = 2995.44 (w), 2957.09 (w), 2889.90 (w), 1717.58 (s), 1639.73 (m), 1505.71 (w), 1478.46 (s), 1446.99 (s), 1354.00 (w), 1319.89 (w), 1295.96 (w), 1245.51 (w), 1150.49 (s), 1101.23 (s), 1047.37 (w), 980.70 (m), 883.79 (w), 814.28 (w), 749.78 (w), 735.08 (w), 654.45 (w).

## Data availability

The data supporting this article have been included as part of the ESI.†

## Conflicts of interest

There are no conflicts to declare.

## Acknowledgements

The authors would like to thank the Natural Sciences and Engineering Research Council (NSERC) for funding, and analysis performed by the École Nationale Supérieure de Chimie de Montpellier (ENSCM) for thermal analysis of the polymers.

## References

- 1 B. Ameduri, Fluoropolymers: The Right Material for the Right Applications, *Chem.-Eur. J.*, 2018, **24**(71), 18830–18841, DOI: [10.1002/chem.201802708](https://doi.org/10.1002/chem.201802708).
- 2 Z. Cui, E. Drioli and Y. M. Lee, Recent Progress in Fluoropolymers for Membranes, *Prog. Polym. Sci.*, 2014, **39**(1), 164–198, DOI: [10.1016/j.progpolymsci.2013.07.008](https://doi.org/10.1016/j.progpolymsci.2013.07.008).
- 3 S. Sukumaran, S. Chatbouri, D. Rouxel, E. Tisserand, F. Thiebaud and T. Ben Zineb, Recent Advances in Flexible PVDF Based Piezoelectric Polymer Devices for Energy Harvesting Applications, *J. Intell. Mater. Syst. Struct.*, 2020, **32**(7), 746–780, DOI: [10.1177/1045389X20966058](https://doi.org/10.1177/1045389X20966058).
- 4 J. Kujawa, S. Boncel, S. Al-Gharabli, S. Koter, A. Kaczmarek-Kędziera, E. Korczyński and A. P. Terzyk, Current and Future Applications of PVDF-Carbon Nanomaterials in





- Energy and Sensing, *Chem. Eng. J.*, 2024, **492**, 151856, DOI: [10.1016/j.ccej.2024.151856](https://doi.org/10.1016/j.ccej.2024.151856).
- 5 Y. Wu, Y. Ma, H. Zheng and S. Ramakrishna, Piezoelectric Materials for Flexible and Wearable Electronics: A Review, *Mater. Des.*, 2021, **211**, 110164, DOI: [10.1016/j.matdes.2021.110164](https://doi.org/10.1016/j.matdes.2021.110164).
  - 6 Y. Roina, F. Auber, D. Hocquet and G. Herlem, EPTFE-Based Biomedical Devices: An Overview of Surgical Efficiency, *J. Biomed. Mater. Res., Part B*, 2022, **110**(2), 302–320, DOI: [10.1002/jbm.b.34928](https://doi.org/10.1002/jbm.b.34928).
  - 7 Y. Roina, F. Auber, D. Hocquet and G. Herlem, EPTFE Functionalization for Medical Applications, *Mater. Today Chem.*, 2021, **20**, 100412, DOI: [10.1016/j.mtchem.2020.100412](https://doi.org/10.1016/j.mtchem.2020.100412).
  - 8 J. Cui, L. Du, Z. Meng, J. Gao, A. Tan, X. Jin and X. Zhu, Ingenious Structure Engineering to Enhance Piezoelectricity in Poly(Vinylidene Fluoride) for Biomedical Applications, *Biomacromolecules*, 2024, **25**(9), 5541–5591, DOI: [10.1021/acs.biomac.4c00659](https://doi.org/10.1021/acs.biomac.4c00659).
  - 9 B. Améduri, The Promising Future of Fluoropolymers, *Macromol. Chem. Phys.*, 2020, **221**(8), 1900573, DOI: [10.1002/macp.201900573](https://doi.org/10.1002/macp.201900573).
  - 10 W. J. Sell and F. W. X. L. V. Dootson, —The Chlorine Derivatives of Pyridine. Part I, *J. Chem. Soc., Trans.*, 1898, **73**(0), 432–441, DOI: [10.1039/CT8987300432](https://doi.org/10.1039/CT8987300432).
  - 11 R. E. Banks, R. N. Haszeldine, J. V. Latham and I. M. Young, 95. Heterocyclic Polyfluoro-Compounds. Part VI. Preparation of Pentafluoropyridine and Chlorofluoropyridines from Pentachloropyridine, *J. Chem. Soc.*, 1965, (0), 594–597, DOI: [10.1039/JR9650000594](https://doi.org/10.1039/JR9650000594).
  - 12 H. Zhiren; H. Zhu; Z. Han; Z. Sun and S. Change Catalytic Synthesis Method and Preparation Device of Pentachloropyridine. *110256334 A*, September 20, 2019.
  - 13 C. B. Murray, G. Sandford, S. R. Korn, D. S. Yufit and J. A. K. Howard, New Fluoride Ion Reagent from Pentafluoropyridine, *J. Fluorine Chem.*, 2005, **126**(4), 569–574, DOI: [10.1016/j.jfluchem.2004.12.013](https://doi.org/10.1016/j.jfluchem.2004.12.013).
  - 14 W. D. G. Brittain and S. L. Cobb, Carboxylic Acid Deoxyfluorination and One-Pot Amide Bond Formation Using Pentafluoropyridine (PFP), *Org. Lett.*, 2021, **23**(15), 5793–5798, DOI: [10.1021/acs.orglett.1c01953](https://doi.org/10.1021/acs.orglett.1c01953).
  - 15 W. D. G. Brittain and S. L. Cobb, Tetrafluoropyridyl (TFP): A General Phenol Protecting Group Readily Cleaved under Mild Conditions, *Org. Biomol. Chem.*, 2019, **17**(8), 2110–2115, DOI: [10.1039/C8OB02899K](https://doi.org/10.1039/C8OB02899K).
  - 16 T. Braun, D. Noveski, M. Ahijado and F. Wehmeier, Hydrodefluorination of Pentafluoropyridine at Rhodium Using Dihydrogen: Detection of Unusual Rhodium Hydrido Complexes, *Dalton Trans.*, 2007, (34), 3820–3825, DOI: [10.1039/B706846H](https://doi.org/10.1039/B706846H).
  - 17 T. Braun, R. N. Perutz and M. I. Sladek, Catalytic C–F Activation of Polyfluorinated Pyridines by Nickel-Mediated Cross-Coupling Reactions, *Chem. Commun.*, 2001, (21), 2254–2255, DOI: [10.1039/B106646C](https://doi.org/10.1039/B106646C).
  - 18 T. Braun, J. Izundu, A. Steffen, B. Neumann and H.-G. Stammer, Reactivity of a Palladium Fluoro Complex towards Silanes and Bu<sub>3</sub>SnCH=CH<sub>2</sub>: Catalytic Derivatisation of Pentafluoropyridine Based on Carbon–Fluorine Bond Activation Reactions, *Dalton Trans.*, 2006, (43), 5118–5123, DOI: [10.1039/B608410A](https://doi.org/10.1039/B608410A).
  - 19 T. J. Fuhrer, M. Houck, C. A. Corley and S. T. Iacono, Theoretical Explanation of Reaction Site Selectivity in the Addition of a Phenoxy Group to Perfluoropyridine, *J. Phys. Chem. A*, 2019, **123**(44), 9450–9455, DOI: [10.1021/acs.jpca.9b06413](https://doi.org/10.1021/acs.jpca.9b06413).
  - 20 C. M. Friesen, A. R. Kelley and S. T. Iacono, Shaken Not Stirred: Perfluoropyridine-Polyalkylether Prepolymers, *Macromolecules*, 2022, **55**(24), 10970–10979, DOI: [10.1021/acs.macromol.2c01310](https://doi.org/10.1021/acs.macromol.2c01310).
  - 21 M. B. Houck, L. C. Brown, R. H. Lambeth and S. T. Iacono, Exploiting the Site Selectivity of Perfluoropyridine for Facile Access to Densified Polyarylene Networks for Carbon-Rich Materials, *ACS Macro Lett.*, 2020, **9**(7), 964–968, DOI: [10.1021/acsmacrolett.0c00298](https://doi.org/10.1021/acsmacrolett.0c00298).
  - 22 L. M. J. Moore, K. T. Greeson, K. A. Stewart, D. A. Kure, C. A. Corley, A. R. Jennings, S. T. Iacono and K. B. Ghiassi, Perfluoropyridine as a Scaffold for Semifluorinated Thiol-Ene Networks with Readily Tunable Thermal Properties, *Macromol. Chem. Phys.*, 2020, **221**(12), 2000100, DOI: [10.1002/macp.202000100](https://doi.org/10.1002/macp.202000100).
  - 23 V. V. Nedel'ko, N. V. Chukanov, B. L. Korsunskiy, T. S. Larikova, S. V. Chapyshev and V. V. Zakharov, Kinetics of the Thermal Decomposition of 2,4,6-Triazido-3,5-Difluoropyridine, *Russ. J. Phys. Chem. B*, 2018, **12**(6), 997–1002, DOI: [10.1134/S199079311806009X](https://doi.org/10.1134/S199079311806009X).
  - 24 C. A. Corley, K. Kobra, A. J. Peloquin, K. Salmon, L. Gumireddy, T. A. Knoerzer, C. D. McMillen, W. T. Pennington, A. M. Schoffstall and S. T. Iacono, Utilizing the Regioselectivity of Perfluoropyridine towards the Preparation of Phenoxyacetylene Precursors for Partially Fluorinated Polymers of Diverse Architecture, *J. Fluorine Chem.*, 2019, **228**, 109409, DOI: [10.1016/j.jfluchem.2019.109409](https://doi.org/10.1016/j.jfluchem.2019.109409).
  - 25 S. Eismeier, A. J. Peloquin, K. A. Stewart, C. A. Corley and S. T. Iacono, Pyridine-Functionalized Linear and Network Step-Growth Fluoropolymers, *J. Fluorine Chem.*, 2020, **238**, 109631, DOI: [10.1016/j.jfluchem.2020.109631](https://doi.org/10.1016/j.jfluchem.2020.109631).
  - 26 P. Qi, J. Wang, L. Wang, Y. Li, J. Jin, F. Su, Y. Tian and J. Chen, Molecularly Imprinted Polymers Synthesized via Semi-Covalent Imprinting with Sacrificial Spacer for Imprinting Phenols, *Polymer*, 2010, **51**(23), 5417–5423, DOI: [10.1016/j.polymer.2010.09.037](https://doi.org/10.1016/j.polymer.2010.09.037).
  - 27 M. Zare, A. Bigham, M. Zare, H. Luo, E. Rezvani Ghomi and S. P. Ramakrishna, An Overview for Biomedical Applications, *Int. J. Mol. Sci.*, 2021, **22**(12), 6376, DOI: [10.3390/ijms22126376](https://doi.org/10.3390/ijms22126376).
  - 28 S. K. Papadopoulou and C. Panayiotou, Assessment of the Thermodynamic Properties of Poly(2,2,2-Trifluoroethyl Methacrylate) by Inverse Gas Chromatography, *J. Chromatogr. A*, 2014, **1324**, 207–214, DOI: [10.1016/j.chroma.2013.11.044](https://doi.org/10.1016/j.chroma.2013.11.044).

